

---

# Highly (200)-Preferred Orientation TiN Thin Films Grown by DC Reactive Magnetron Sputtering

Li Haiyi\*, Liu Yongzhi, Gao Bingxiang, Xie Liqiang

Department of Physics and Hydraulic Engineering, Gansu Normal University for Nationalities, Hezuo, P R China

## Email address:

Lihaiyi6018@sina.com (Li Haiyi)

\*Corresponding author

## To cite this article:

Li Haiyi, Liu Yongzhi, Gao Bingxiang, Xie Liqiang. Highly (200)-Preferred Orientation TiN Thin Films Grown by DC Reactive Magnetron Sputtering. *American Journal of Physics and Applications*. Vol. 5, No. 3, 2017, pp. 41-45. doi: 10.11648/j.ajpa.20170503.12

Received: April 5, 2017; Accepted: June 13, 2017; Published: June 27, 2017

---

**Abstract:** Titanium nitride ( $\text{TiN}_x$ ) thin films were prepared on Si(111) substrates by DC reactive magnetron sputtering. The influence of chamber pressure on the lattice constants, grain size, surface morphologies, conductivity and visible-near infrared reflectance of  $\text{TiN}_x$  thin films were investigated. It is shown that the main component of the thin films is cubic TiN with (200) preferred orientation. The resistivity of the TiN thin film increase along with the increase of the chamber pressure, whereas the lattice constants and average reflectance within near infrared range of the TiN thin film decrease gradually. For all the TiN films, there is a minimum reflectance around 455nm.

**Keywords:** TiN Thin Film, Magnetron Sputtering, Chamber Pressure, Lattice Constant, Optical Reflectance

---

## 1. Introduction

Almost all elements can bond with nitrogen to form binary nitride compounds, among them titanium nitride (TiN) is an interesting material [1]. Because of its uncommon set of physical, chemical, and mechanical properties, such as high thermal stability, good chemical inertness, high hardness, low electrical resistivity and superior irradiation resistance, TiN films have been widely used for various applications including hard coatings on tools. TiN is a promising material because it can be used to cut tools wear-resistant coatings, diffusion barriers [2], photo-thermal solar energy conversion layer [3], semi-transparent contacts in solar cells [4] due to it possesses many interesting physical and chemical properties, such as high hardness, high melting point, high chemical stability, good electrical conductivity (around  $30\mu\Omega\cdot\text{cm}$ ), high optical reflectivity (its colors varying from gold to dark brown) that are beneficial for applications in high temperature heterogeneous catalysis [5, 6] and so on. What is more, TiN has a high reflectance in the infrared (IR) range and high transmittance in the visible range when the thickness of the films is less than 30 nm, So it is usually used as optical selective coatings [7, 8]. The electrical and optical properties of TiN films depend strongly on composition (Ti/N ratio), and

structure of, which are established by the preparation method and process conditions [9, 10]. There are many articles describing various surface treatments or coatings that could be deposited on prosthesis to increase their corrosion resistance, osseointegration and biocompatibility and to reduce the wear rates and the resulting debris quantity and size. Several deposition techniques have been applied in the deposition of TiN films, such as metal-organic chemical vapor deposition (MOCVD), plasma enhanced chemical vapor deposition (PECVD), electron cyclotron resonance plasma chemical vapor deposition (ECRCVD), direct current (DC) reactive magnetron sputtering, low temperature plasma treatment with  $\text{N}_2$  as plasma source etched the obtained films to produce the nanostructured TiN-based thin films [11]. In this work, TiN thin films were prepared on silicon substrates by DC reactive magnetron sputtering to improve the resistivity and the optical reflectivity of TiN thin films by changing the chamber pressure. In order to acquire the optimized deposition process parameters of TiN thin films with better properties, the influence of chamber pressure on lattice constants, grain sizes, surface morphologies, conductivity and visible-near infrared reflectance of TiN thin films were investigated.

## 2. Experimental Procedure

The TiN thin films were deposited on silicon substrates by DC reactive magnetron sputtering. The size of the chamber was 55cm (diameter)×34cm(height) and the chamber was pumped down to  $1.0 \times 10^{-5}$ Pa by a 400Hz turbo molecular pump before the mixed gas inletting. The TiN thin films The target was a 99.99% pure Ti with a diameter of  $\Phi=100$ mm. The distance of target to substrate is 60cm. The p-type Si (111) wafer, resistivity of 8-12 $\Omega \cdot$ cm, were subsequently cleaned by hydrofluoric acid, acetone, alcohol, deionized water in a ultrasonic cleaner for 10min(each step) and then blew by high-pressure pure N<sub>2</sub> gas. The flow rate of N<sub>2</sub> gas and Ar gas (both purity of 99.999%) were 10 and 30sccm, respectively. The TiN thin films were then deposited onto Si (111) substrates at 500°C with fixed current (0.35A) for a lasted deposition time of 60min. The chamber pressure varied within

0.3-1.5Pa by adjusting the pumping speed via the opening control of throttle valve.

## 3. Results and Discussion

XRD patterns of DC reactive sputtered TiN films prepared under various chamber pressure is shown in Figure 1. The TiN(111), TiN(200) and TiN(220) peaks at  $2\theta=36.9^\circ, 42.9^\circ, 62.1^\circ$  are observed, the intensity of (111) and (220) peaks are much weaker than that of (200) peak for all samples, and one can find Si(111) peaks at  $2\theta=28.4^\circ$  when the chamber pressure varied within 0.3-1.5Pa. From the XRD patterns, it can be found that all the TiN films are polycrystalline cubic structure with (200) preferred orientation. The intensity of (200) diffraction peaks depends on the chamber pressure, when the chamber pressure increase from 0.3 to 1.5Pa, the intensity of (200) peaks decrease.

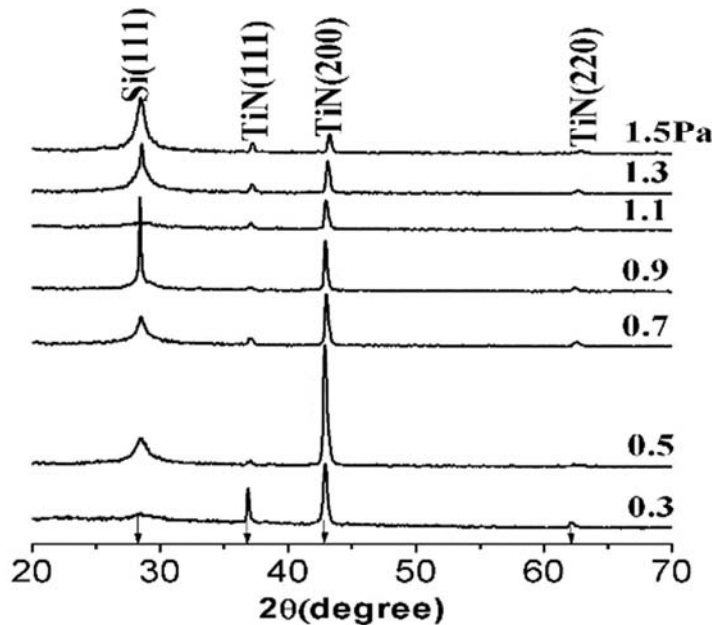


Figure 1. XRD patterns of DC sputtered TiN films prepared under various chamber pressure.

The lattice constant of the cubic structure TiN films with (200) preferred orientation can be calculated from the X-ray diffraction angle( $\theta$ ) using the following formulae:

$$2d \sin \theta = n\lambda \tag{1}$$

and

$$\frac{1}{d^2} = \frac{(h^2 + k^2 + l^2)}{a_0^2} \tag{2}$$

where  $a_0$ ,  $d$ ,  $\theta$ ,  $n$ ,  $\lambda$ , and  $hkl$  are the lattice constant, the distance of the two adjacent (200) planes, the diffraction angle, the order of diffraction, the wavelength of the radiation and the miller index. The calculated lattice constants are listed in table 1. It is found that the lattice constant decrease gradually as the

chamber pressure increase, and that is why the (200) peaks are right-moved slightly.

The average grain size of the TiN films with (200) preferred orientation can also be calculated from the X-ray diffraction angle ( $\theta$ ) by Scherer’s formula:

$$GS = \frac{k\lambda}{B \cos \theta} \tag{3}$$

Here B is the full width at half-maximum (FWHM) of the (200) peak, k is a constant varied from the range of 0.89-1.39. The average grain size of the TiN films are listed in table 1 when the constant k is set to 1.1. The surface morphology of the TiN films ranging from 0.3Pa to 1.5Pa are shown in Figure 2.

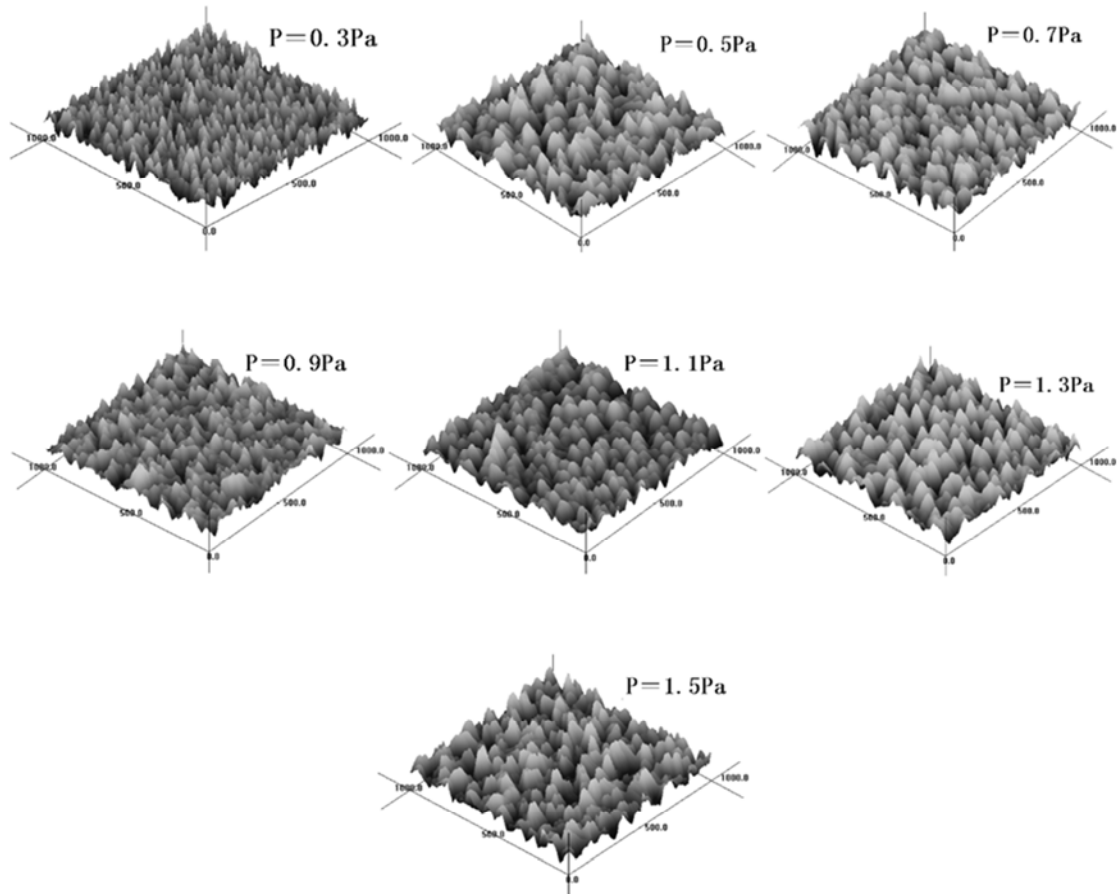


Figure 2. AFM images of TiN films deposited under various chamber pressure.

Table 1 displays the root mean square (Rms) surface roughness and average grain size of the films detected by AFM off-line software. The Rms surface roughness at 0.3Pa was 2.06nm, whereas the Rms surface roughness at 1.5 Pa was 6.89nm, that is correspond clearly to Figure 2. What is more, the grain size detected by AFM off-line software shown in table 1, close to that calculated by Scherer’s formula (k=1.1) within a maximum relative error 9.57%.

The resistivities of the TiN films can be calculated by the

following formula

$$\rho = R_{\square} \cdot d \tag{4}$$

Where  $\rho$  is resistivity,  $R_{\square}$  and  $d$  are sheet resistance and the thickness of the films measured by four-point probe and step profilometer, respectively. The thickness, sheet resistance and calculated resistivity were listed in table 1.

Table 1. Experimental results of TiN thin films under different chamber pressure.

chamber pressure P/Pa	thickness d /nm	lattice constants $a_0$ /nm	mean grain size (by XRD) /nm	mean grain size (by AFM) /nm
0.3	132	0.421	31.42	30.01
0.5	128.8	0.421	35.49	35.60
0.7	127.3	0.420	39.55	37.64
0.9	125.1	0.420	39.61	41.10
1.1	112.2	0.420	31.15	28.97
1.3	111.9	0.419	31.00	29.53
1.5	108.3	0.418	32.30	29.21

Table 1. Continue.

rms roughness /nm	sheet resistance $R_{\square}$ /Ω	resistivity $\rho$ /μΩ·cm	mean optical reflectivity within 760-1000nm
2.06	2.56	33.8	0.85
5.97	7.42	95.6	0.78
3.50	16.69	212.5	0.71
5.72	17.32	216.7	0.63
6.63	19.78	221.9	0.52
2.85	22.11	247.4	0.36
6.89	66.5	720.1	0.33

The resistivity of TiN thin films vs chamber pressure curve was shown in Figure 3. The minimum and maximum resistivity are  $33.8\mu\Omega\cdot\text{cm}$  (close to that of the bulk TiN) and  $720.1\mu\Omega\cdot\text{cm}$  corresponding to the chamber pressure are 0.3 and 1.5Pa, respectively. It is shown in Figure 3 that the resistivity of TiN thin films depends on the chamber pressure and increase gradually as the chamber pressure increase within 0.3-1.5Pa.

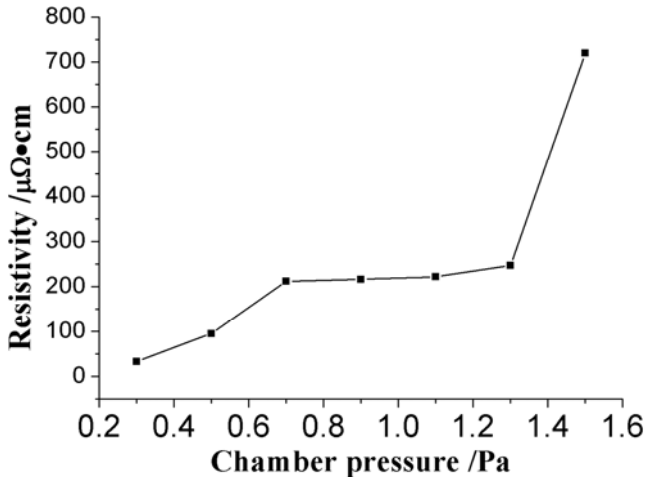


Figure 3. The resistivity of TiN thin films vs the chamber pressure.

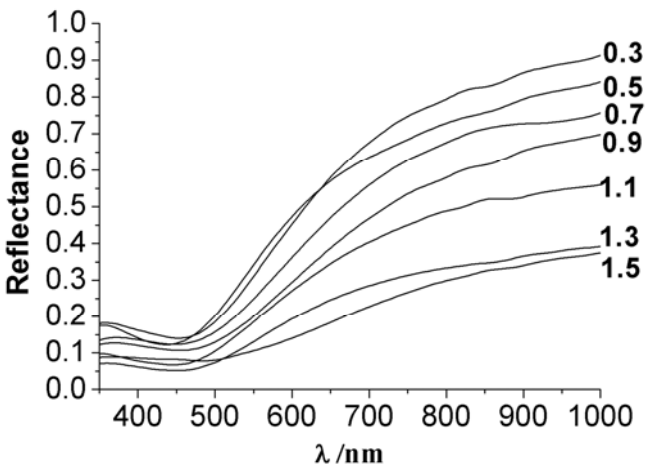


Figure 4. The reflective spectra of TiN thin films.

The optical properties of the fabricated films were analyzed by measuring the reflection spectrum in the wavelength range of 350-1000nm using the spectrophotometer. The typical reflection spectrum of the films deposited at various chamber pressure are shown in Figure 4. The minimum reflectivity of the films existed in the range of 450-460nm that agree well with the results reported by A. Lousa in Ref. [12]. The average reflectivity of the films in the near infrared range (wavelength  $\lambda=760\sim 1000\text{nm}$ ) were listed in table 1 when the chamber pressure increases from 0.3Pa to 1.5Pa, which means the reflectivity of the films decreasing with increasing the chamber pressure.

## 4. Conclusion

In this paper, TiN thin films were deposited on silicon substrates by DC reactive magnetron sputtering to improve the resistivity and the optical reflectivity of TiN thin films by changing the chamber pressure. The result is shown that the structural, electrical and optical properties of the TiN thin films depend clearly on the chamber pressure. All films are polycrystalline cubic structure. The grain size obtained by XRD and AFM are coincident. The Rms surface roughness at 0.3Pa was 2.06nm, whereas the Rms surface roughness of the TiN thin films at 1.5 Pa was 6.89nm. The lattice constant and optical reflectivity of the films decrease, while the resistivity of the films increase, as the chamber pressure increase from 0.3Pa to 1.5Pa. The lowest resistivity was  $33.8\mu\Omega\cdot\text{cm}$  (close to that of the bulk TiN) when the chamber pressure is 0.3Pa, correspondingly, the highest average reflectivity in the near infrared range (wavelength  $\lambda=760\text{-}1000\text{nm}$ ) of the TiN thin films was 0.85.

## Acknowledgments

The current work is supported by Gansu Scientific Research Projects in Universities (NO. 2016B-107), Longyuan Talent Support Program of Gansu Province (NO. 2014C-74) and Principal Scientific Research Fund of Gansu Normal University for Nationalities (NO. GSNUXM16-10).

## References

- [1] Jianyun Zheng, Yanhong Lv, Shusheng Xu, et al. "Nanostructured TiN-based thin films by a novel and facile synthetic route". *Materials and Design* 2017, pp: 142–148.
- [2] Jijun Yang, Mingjin Peng, Jiali Liao, et al. "Effect of N<sub>2</sub> gas injection parameters on structure and properties of TiN thin films prepared by reactive gas pulse sputtering". *Surface & Coatings Technology*, 2017, pp: 391–397.
- [3] Huang J H, Ma C H, Chen H. "Effect of Ti interlayer on the residual stress and texture development of TiN thin films deposited by unbalanced magnetron sputtering". *Surface & Coatings Technology*, 2006, Vol. 201(6)pp: 3199-3204.
- [4] Mubarak A, Hamzah E, Toff M R M, et al. "Study of macrodroplet and growth mechanisms with and without ion etchings on the properties of TiN coatings deposited on HSS using cathodic arc physical vapour deposition technique". *Materials Science and Engineering A*, 2008, 474pp: 236-242.
- [5] Wang J M, Liu W G, Mei T. "The effect of thermal treatment on the electrical properties of titanium nitride thin films by filtered arc plasma method". *Ceramics International*, 2004, Vol. 30(7)pp: 1921-1924.
- [6] Suharyanto, Shinichiro M, Yoshio S, et al. "Secondary electron emission of TiN-coated alumina ceramics". *Vacuum*, 2007, Vol 81(6)pp: 799-802.

- [7] Tung Sheng Y, Jenn Ming W, Long Jang H, et al. "the properties of TiN thin film deposited by pulsed direct current magnetron sputtering". *thin solid films*, 2008, 516pp: 7294-7298.
- [8] Gaoling Zhao, Tianbl Zhang, Tao Zhang, et al. "Electrical and Optical Properties of Titanium Nitride Coatings Prepared by Atmospheric Pressure Chemical Vapor Deposition". *Journal of Non-Crystalline Solids*, 2008, 354pp: 1272-1275.
- [9] An-NiWang, Jia-Hong Huang, Haw-Wen Hsiao, et al. "Residual stress measurement on TiN thin films by combining nanoindentation and average X-ray strain (AXS) method". *Surface & Coatings Technology*, 2015, pp: 43-49.
- [10] Jeong An Kwon, Min-Su Kim, "Dong Yun Shin. First-principles understanding of durable titanium nitride (TiN) electrocatalyst supports". *Journal of Industrial and Engineering Chemistry*, 2017, 49 pp: 69-75.
- [11] Jianyun Zheng, Yanhong Lv, Shusheng Xu. "Nanostructured TiN-based thin films by a novel and facile synthetic route". *Materials and Design*, 2017, 113pp: 142-148.
- [12] Lousa A, Esteve J, Pmejia J, et al. "Influence of Deposition Pressure on the Structural Mechanical and Decorative Properties of TiN Thin Films Deposited by Cathodic Arc Evaporation", *Vacuum*, 2007, 81pp: 1507-1510.